Title: The secret life (cycle) of temperate bacteriophages

Alfred Fillol-Salom[1,†], Rodrigo Bacigalupe[2,3,†], Suzanne Humphrey[1], Yin Ning Chiang[4], John Chen[4,*], José R Penadés[1,5,*].

[1]Institute of Infection, Immunity and Inflammation, College of Medical, Veterinary and Life Sciences, University of Glasgow, Glasgow, G12 8TA, UK

[2]Dep. Ciencias Biomédicas, Universidad CEU Cardenal Herrera, 46113, Moncada, Spain.

[3]The Rega Institute for Medical Research, KU Leuven, 3000, Leuven, Belgium.

[4]Department of Microbiology and Immunology, Yong Loo Lin School of Medicine, National University of Singapore, 5 Science Drive 2, Singapore.

[5]MRC Centre for Molecular Bacteriology and Infection, Imperial College London, SW7 2AZ, UK.

[†]These authors contributed equally.

Running title: Life cycle of temperate bacteriophages

Keywords: Lateral transduction, *Salmonella enterica*, pathogenicity islands, evolution, virulence, gene transfer, transduction, phage, P22.

[*]Corresponding authors: John Chen
Department of Microbiology and Immunology
Yong Loo Lin School of Medicine
National University of Singapore
e-mail: miccjy@nus.edu.sg

José R. Penadés
Centre for Molecular Bacteriology and Infection
Imperial College London
e-mail: j.penades@imperial.ac.uk

Abstract

Lysogenic induction ends the stable association between a bacteriophage and its host, and the transition to the lytic cycle begins with prophage excision followed by DNA replication and packaging (ERP) – a temporal program that is considered universal for most temperate phages. Here we report that the long-standing ERP program is an artefact of the experimentally favoured *Salmonella* phage P22 tsc_2*29* heat-inducible mutant, and that wild-type P22 actually follows a replication-packaging-excision (RPE) program. We found that unlike P22 tsc_2*29*, P22 delayed excision to just before it was detrimental to phage production. Thus, at minimal expense to itself, P22 has tuned the timing of excision to balance propagation with lateral transduction, powering the evolution of its host through gene transfer in the interest of self-preservation.

One Sentence Summary: Genetic analyses propose a new life cycle for temperate bacteriophages.

Bacteriophages (phages) are viruses that infect and replicate within bacteria. They are the most diverse and abundant biological entities on the planet, and they play an important role in controlling populations of bacteria that they exploit and kill. Yet their existence is tied to the success and survival of the hosts that they parasitize, and in the interest of self-preservation, phages can act as powerful agents of microbial adaptation and evolution by means of their ability to transfer bacterial DNA (encoding virulence factors and antibiotic resistance) from one bacterium to another by a process known as genetic transduction.

Phages are obligate intracellular parasites that follow two different life cycles. In the lysogenic cycle, temperate phages reproduce by integrating their genomes into the bacterial host chromosome where they persist in a dormant state as a prophage and replicate passively as part of the bacterial chromosome during cell division. Infectious phage particles are produced in the lytic cycle, following host cell infection or prophage induction from the lysogenic cycle. Viral DNA replication first occurs bidirectionally, followed by a switch to rolling-circle replication that generates long DNA concatemers of multiple phage genomes (*1*, *2*). The concatemeric DNA is packaged by the phage terminase enzyme (a hetero-oligomer of small and large terminase proteins), which recognizes a phage-specific packaging site (*pac* or *cos*) and cleaves the DNA to begin processing the genome into newly formed phage heads (*3*, *4*). To complete DNA packaging, *pac*-type terminases make a nonspecific terminal cut when a capsid headful (slightly longer than a genome unit length) has been reached (*5*, *6*), while *cos*-type terminases require a second *cos* site to make the second cut (*7*), forming infectious phage particles that are released during bacterial cell lysis. It is also during this process that transducing particles are formed, when bacterial DNA is packaged into phage heads.

Lysogeny is generally very stable when maintained by sufficient levels of phage repressor, but prophages can switch to the lytic cycle when their hosts begin to deteriorate. They do so by exploiting the bacterial SOS response, which is a global repair pathway that responds to DNA damage and serves as a proxy for the health of the host. Under normal conditions, the SOS-inducible genes are negatively regulated by the bacterial LexA repressor.

After a cell experiences DNA damage, the bacterial RecA protein becomes activated by single-stranded DNA and acts as a co-protease to stimulate the self-cleavage of LexA (*8*, *9*). This response is rapid and reversible, and complete LexA cleavage occurs in less than 5 minutes so that minor insults to the cell can be repaired in a timely manner (*10*). Many phage repressors, such as those of phages λ and P22, mimic the structure of LexA and are also induced to self-cleavage by activated RecA (*11*). However, phage repressors are cleaved far slower than LexA and take up to 30 minutes or longer to reach levels that are low enough to de-repress phage lytic genes (*10*, *12*, *13*). Presumably, this is to ensure that lysogenic induction only occurs in cells that have received prolonged damaging exposure and are not expected to survive. Alternatively, the SOS response can be bypassed entirely with prophages that carry temperature-sensitive repressor (ts*c*) mutations. For instance, thermal induction of λ and P22 ts*c* mutants was the experimental method of choice for prophage de-repression because it occurred within minutes and the cultures were regarded as more synchronized (*2*, *14*).

After lysogenic induction, prophages are presumed to excise (and circularize) early as the first step in the temporal program of excision–replication–packaging (the ERP cycle; Fig. S1). This sequence of events is widely accepted and believed to be universal for all integrated prophages because it was thought that DNA packaging prior to excision would split the viral genome and prevent the production of infectious phage particles. Also, experimental support from λ and P22 studies showed that the proteins involved in excision (integrase and excisionase) were early gene products that appeared soon after phage infection or thermal induction of ts*c* mutants (*2*, *14*-*16*). However, that appears to be the extent of the data on excision timing, and there seems to be no direct evidence that validates the model for early excision (*17*). Further complicating the matter, recently we found that some staphylococcal prophages delay excision until later in their lytic cycle (*18*), and others have shown that some *Salmonella* prophages likely do the same (*19*). Therefore, the timing of prophage excision turns out to be an unresolved part of what was thought to be a well-defined phage life cycle.

While the distinction between early or delayed prophage excision might seem minor, it has profound evolutionary consequences because only the latter is predicted to result in lateral transduction (*18*).

Phage-mediated gene transfer is known to occur by three different mechanisms: specialized (ST), generalized (GT), and lateral transduction (LT). In the first, specialized-transducing particles are formed when viral and bacterial DNA hybrid molecules are encapsidated following aberrant prophage excision events (*20*). The mechanism is considered specialized because it is limited to the transfer of bacterial genes immediately adjacent to the integrated prophage. In the second, generalized-transducing particles are formed when *pac*-type terminases recognize *pac* site homologs in host DNA and initiate packaging by the headful mechanism (*21*). The mechanism is regarded as generalized because any bacterial DNA can be packaged and transferred in this manner. In the recently discovered LT, transducing particles are formed when DNA packaging initiates from the bona fide *pac* sites of prophages that have delayed excision and are still attached to the bacterial chromosome (*18*, *22*). The headful mechanism fills the first capsid with part of the prophage genome and continues through the adjacent bacterial chromosome for up to seven or more successive capsid headfuls. To prevent splitting the integrated viral genome in two, bidirectional *in situ* replication (prior to DNA packaging) creates sufficient genomic redundancy to enable LT and phage maturation to proceed in parallel. Together, this results in a mode of transduction that produces normal phage titers and transfers bacterial chromosomal DNA at frequencies far greater than previously observed for known mechanisms of host gene transfer.

Much of our current understanding of fundamental phage biology derives from the body of work on the archetypal *Salmonella pac*-type phage P22. In those studies, P22 ts*c* mutants were used for lysogenic induction because they were otherwise regarded as WT. Here we found that P22 follows two different temporal programs to produce infectious phage particles, depending on the method of lysogenic induction. Thermal induction of a P22 ts*c* mutant resulted in early prophage excision and the classical ERP program. SOS induction of P22

resulted in delayed prophage excision, DNA replication and packaging *in situ*, and LT (see scheme in Fig. S1). These results propose a new series of events in the life cycle of temperate prophages and show that early excision was an unnatural consequence of an experimental system and that delayed excision leading to LT are naturally parts of the phage life cycle.

Results

Lysogenic induction differs by thermal induction or the SOS response

As we noted earlier, prophage de-repression by thermal induction was known to occur much more rapidly than SOS induction (*2*, *14*). This disparity in timing suggested that the heat-induced temporal program was either intact (but shifted ahead of schedule) or it was unnatural. To distinguish these possibilities, we performed transcriptional profiling of P22 and P22 tsc_2*29* (*23*). For phage infection, a non-lysogenic derivative of *Salmonella enterica* LT2 that was cured of all four of its resident prophages was infected with P22. For prophage induction, lysogenic strains were grown at permissive temperature (32°C) and for thermal induction the P22 tsc_2*29* lysogen was shifted to 42°C or to trigger the SOS response the P22 lysogen was treated with mitomycin C. Following thermal induction (for 30 minutes), the cultures were returned to 32°C because P22 (WT and tsc_2*29*) forms mostly particles that lack functional tails when incubated at high temperatures for prolonged periods (*24*). Total RNA was harvested at 0, 30, 60, and 90 minutes after infection or induction for RNA-sequencing analysis. We found that following SOS induction of the P22 prophage, most viral transcripts did not appear until 30 to 60 minutes and only reached maximal levels by 90 minutes, which was consistent with a gradation effect caused by the inactivation of the P22 repressor over time. In contrast, total viral transcripts reached maximal levels early (before 30 minutes) following infection, due to the total lack of repressor in naïve cells (Fig. 1). Surprisingly, thermal induction of P22 tsc_2*29* also resulted in maximal viral RNA levels before 30 minutes and mirrored the RNA transcript profiles of lytic infection, suggesting that the pool of P22 tsc_2*29* repressor was inactivated so completely and rapidly that the viral genome was de-regulated to the extent as it was during

lytic infection. Therefore, compared to SOS induction of P22, the P22 tsc_2*29* program was shifted early, compacted to a small window of time, and no longer temporally regulated.

In the bottom strand, RNA transcripts of the integrase and excisionase genes (*int* and *xis*) appeared early (before 30 minutes) after P22 infection or thermal induction of P22 tsc_2*29*, but much later (between 30 and 60 minutes) after SOS induction of P22 (Fig. 1). These results were consistent with the P22 tsc_2*29* literature and suggested that P22 tsc_2*29* excises much earlier than P22 following induction. To correlate the appearance of *int* and *xis* transcripts with prophage excision, the lysogenic strains were induced under the same conditions as above and total chromosomal DNA was isolated for whole-genome sequencing. Here we included ES18, a *Salmonella pac*-type phage with an unrelated DNA-packaging module, to broaden the scope of our study. At each time point, we compared the number of sequencing reads corresponding to empty prophage attachment sites (*att*B) with the number of reads covering the *att*L site (the left end of the integrated prophage) and represented the results as the percentage of integrated prophage.

Prior to induction, spontaneous excision was observed for P22 tsc_2*29* (Fig. S2), owing to the general leakiness of transcription in the mutant (Fig. 1). Following lysogenic induction, the percentage of integrated P22 tsc_2*29* declined before 30 minutes, while those of P22 and ES18 remained steady before decreasing between 30 to 60 minutes (Fig. S2). These results were consistent with the transcriptomics data and confirmed that lysogenic induction by temperature shift or the SOS response results in early or delayed excision, respectively.

Thermal induction results in an unnatural temporal program

Though the percentage of integrated P22 decreased from 30 to 60 minutes after SOS induction, it began to change course and increased after 60 minutes (Fig. S2). This curious result suggested that the P22 prophage was either reintegrating or replicating prior to excision. Previously, we had a similar observation with staphyloccocal prophages and found that *in situ* replication caused the late increase in the percentage of integrated prophage (*18*), so we constructed a deletion mutant of the P22 *pri* gene that initiates bidirectional (theta) replication

and tested it for excision as above. Shown in Figure S2, the percentage of integrated P22 (Δ*pri*) now decreased from 60 to 90 minutes, confirming that P22 excision occurs late and that P22 replicates before excision.

To confirm that P22 replicates *in situ*, we checked for escape replication, which is a phenomenon that occurs when prophage replication starts before excision and amplifies the bacterial genome flanking the integrated prophage. For example, P22 prophage mutants that are "locked-in" (unable to excise) have been shown to initiate replication *in situ* and amplify neighbouring regions of the chromosome (*25*). To test for this, we first deleted the *int* or *xis* genes to generate P22 mutants that are unable to excise to serve as controls for escape replication. Then we infected the non-lysogenic strain with P22 or induced the lysogenic derivatives of P22 (WT, Δ*pri*, Δ*int*, and Δ*xis*) with mitomycin C or P22 tsc_2*29* with thermal induction and collected the total chromosomal DNA for whole-genome sequencing. At each time point, we quantified the reads corresponding to P22 and the host DNA adjacent to the *att*B$_{P22}$ site and represented them as the coverage relative to the average of the entire genome. P22 infection showed early (before 30 minutes) and strong amplification of phage DNA (Fig. 2), which was consistent with the P22 literature (*2*, *14-16*). SOS induction of the P22 lysogenic derivatives showed clear amplification of phage DNA later in the lytic cycle (Fig. 2), except for the P22 (Δ*rep*) mutant, which remained flat at all time points because it was unable to replicate.

P22 DNA amplification initiated between 30 to 60 minutes and was much more robust by 90 minutes when episomal replication occurred. By comparison, the P22 (Δ*int*) and P22 (Δ*xis*) mutants showed similar levels of phage DNA amplification at early times, but not at 90 minutes because they were not capable of episomal replication. Consistent with their inability to excise, amplification of the flanking bacterial DNA was higher for P22 (Δ*int*) and P22 (Δ*xis*) than P22 by 90 minutes (Fig. 2). These results confirm that P22 initiated replication while integrated and amplified the adjacent host DNA.

Compared to SOS induction of P22, thermal induction of the P22 tsc_2*29* mutant resulted in an altered replication pattern with much greater levels of phage DNA amplification at 0 and 30 minutes. It is likely that the higher levels of phage DNA amplification observed were due to early-onset episomal replication of the spontaneously-excised genomes (Fig. 2; Fig. S1). Interestingly, the P22 tsc_2*29* mutant also amplified flanking bacterial DNA earlier (before 30 minutes) than P22 (Fig. 2), which was probably due to rapid de-repression of the entire P22 tsc_2*29* genome from thermal induction (Fig. 1).

Taken together, these results show that thermal induction resulted in the classical ERP program where the prophage genome separated early from the bacterial chromosome before replication, while SOS induction resulted in delayed prophage excision and an RPE program. Similar results were also observed for the ES18 prophage (Fig. S3), indicating that other *Salmonella* prophages initiate replication *in situ* as well. Therefore, the heat-induced temporal program was not just early, but it is unnatural as well.

P22-mediated lateral transduction by SOS induction

P22 is not known to engage in LT. Early studies that characterised theoretical modes of phage transduction found that transductions with lysates from P22 tsc_2*29* lysogens (that were heat-induced for longer than 75 minutes) did not support the models that most resembled LT (*26*). The main processes of LT are late prophage excision that link to DNA replication and packaging *in situ*. Since thermal and SOS induction cause very different temporal programs, we reasoned that they would result in equally different outcomes in terms of *in situ* packaging and LT. To test for *in situ* DNA packaging, we inserted tetracycline resistance markers (*tet*A) on both sides of the P22 *att*B site, in the directionality of phage packaging (*tet*A^F) and in the opposite direction (*tet*A^R), to serve as proxies for bacterial gene transfer. The locations of the markers were chosen in reference to the P22 *pac* site, which is embedded in the center of the small terminase gene (*ter*S) and directs packaging unidirectionally toward the 3' end (*4*, *27*). The headful packaging mechanism reaches capacity (~105% of the genome unit length) around 44kb, and the markers were placed so that there would be sufficient flanking DNA for

homologous recombination in the non-lysogenic recipient. Additional markers in the directionality of terminase packaging were also introduced at positions marking successive capsid headfuls to determine how much of the bacterial chromosome could be mobilized from a single lysogen by the highly processive DNA packaging machinery. These markers were also used for ES18 since both phages integrate at the same *att*B site (*28*). Non-lysogenic strains (deleted for the P22 *att*B site) carrying each of these markers were infected with P22 and ES18 to assess GT or strains lysogenic for P22 tsc_2*29*, P22, and ES18 were induced to assess LT and the resulting lysates were tested as donors of tetracycline resistance to *S. enterica.*

We found that after SOS induction of the P22 lysogens, up to seven headfuls (>300 kb) were transferred at frequencies 2-3 orders of magnitude greater than by GT and remained greater than GT for up to twelve headfuls (>500 kb) (Fig. 3a). This P22-mediated LT occurred by the headful mechanism during lysogenic induction (Fig. S5), rather than by the superinfection of lysogenic strains by phages that were released early after SOS induction (Fig. S6). Similar results were also observed for ES18-mediated LT (Fig. S4). In contrast, after thermal induction of the P22 tsc_2*29* lysogen, the transfer frequencies of the first two *tet*A^F markers were significantly lower than those seen for after SOS induction of P22 (Fig. 3b). This result likely explains why earlier studies did not observe LT with the P22 tsc_2*29* mutant: the low LT frequencies were further obscured by the high ratio of tail-defective P22 particles from prolonged thermal induction. Taken together, these results show that P22 and ES18 engage in LT and transmit a large section of the *Salmonella* chromosome during SOS (but not thermal) induction. To expand our studies even further, we tested for LT in *Enterococcus faecalis* strain with phage pp1 (*29*). As shown in Fig. S7, following SOS induction, prophage pp1 transferred *tet*M markers in the directionality of packaging at much higher frequencies than a marker in an unlinked location in the chromosome, showing that LT occurs in *E. faecalis* and it is a widespread and universal mechanism of gene transfer.

For a more direct visualization of LT, we purified P22 particles resulting from SOS induction and extracted the DNA for sequencing. The reads were quantified and mapped to the bacterial chromosome (NC_003197) and quantified based on coverage. We found that 96.5% of the reads of bacterial origin mapped to a 590 kb region in the directionality of packaging by P22-mediated LT. The remaining reads of bacterial origin were randomly distributed along the whole genome, which was indicative of GT (Fig. 4a). The individual headfuls could be visualized by a step down in DNA packaging efficiency for each successive headful, corresponding to each re-initiation of DNA packaging by the processive terminase enzyme (Fig. 4b). Each step was approximately 44 kb in length, which matched the predicted headful capacity for P22.

The timing of prophage excision is tuned for lateral transduction in the newly identified phage RPE cycle

Because early excision (by the P22 tsc_2*29* mutant) resulted in high phage titers and low levels of LT, the opposite should be true for very late excision. This was indeed the case, as the P22 (Δ*int*) and P22 (Δ*xis*) single mutants or a P22 (Δ*int-xis*) double mutant resulted in much lower phage titers and higher levels of LT than WT P22 (Fig S8). Matching results were obtained when different ES18 mutants were also analysed (Fig. S8). Therefore, we wondered if there was a cost to P22 for delayed excision in terms of phage production. To test this, we designed a system in which prophage excision was tightly regulated and inducible. The P22 *int-xis* double mutant was complemented with a plasmid expressing the *int* and *xis* genes under the control of an arabinose-inducible promoter. To test for LT, we used the *tet*A^F marker located in the second P22 headful, thus avoiding any possible interference with ST. This strain was SOS-induced with mitomycin C [time (t) = 0 min] and arabinose was added at different time points ranging from 0 to 4h (after mitomycin C) for *int-xis* expression. As expected, early expression (t=0 mins) of the *int* and *xis* genes after SOS induction produced high phage titers but significantly reduced LT, while very late expression (t=240 mins) resulted in low phage titers and high levels of LT (Fig. 5). Interestingly, *int-xis* expression at 0 to 60 mins maintained

P22 titers at the same high levels, with only a minor decline at 90 mins. At 120 to 240 mins, the phage titer declined rapidly, presumably because *in situ* DNA packaging compromised the integrity of the prophage genomes. By comparison, *int-xis* expression at 90 to 240 mins was optimal for LT. These results indicate that a delay in excision up to 60 to 90 minutes imposes a minimal cost to phage production and allows P22 to engage in LT. Thus, P22 prophage excision occurs in a narrow window of time that balances maximum phage production with LT.

Discussion

Phages have traditionally been viewed as selfish elements that exploit bacteria for their reproduction and spread in nature. The ERP program underscored this self-serving lifestyle because early prophage excision severed the connection to the bacterial cell and opened the way for unchecked viral propagation without any regard for the host. This sequence of events was based on the work from early studies with archetypal phages P22 and λ, and it has stood as the only life cycle described for temperate phages following lysogenic induction. However, phages are perhaps not as selfish as once presumed, and here we found that the temperate phage life cycle is much more intimate and mutually beneficial than previously understood. Our results demonstrate that temperate phages do not follow the ERP program, but instead follow an RPE program, so that the prophage remains connected to the host chromosome for most of its life cycle following lysogenic induction. It does this by starting with *in situ* replication, which generates multiple copies of the integrated prophage to create genomic redundancy. Once the DNA packaging machinery is assembled, *in situ* packaging initiates from some of the integrated prophages and excision occurs from some of the others, so that the production of lateral-transducing particles occurs during normal phage maturation (see scheme in Fig. S1c).

Lysogenic protection and “morons” are the most common examples of benefits that temperate prophages provide to their bacterial hosts. In the first, prophages provide immunity against infection by other phages encoding identical or similar repressors. Phage morons are accessory genes that are not required for the phage life cycle but can increase the fitness of

the lysogenic cell (*30*). Importantly, defective prophages can still provide the benefits of lysogenic protection and morons, while prophages must be intact and functional to impart the benefits of LT. Thus, the RPE cycle (including LT) is an evolutionary force that preserves prophage integrity so that they remain intact and able to propagate. Moreover, we also propose here that LT is not just a universal mechanism of gene transfer, but an event that forms an intrinsic part of the life cycle of temperate *pac* prophages. We have recently demonstrated that phages benefit from GT (*31*), and our unpublished results demonstrate that phages benefit even more from LT. Thus, once prophage genomes integrate into the bacterial chromosome, their fates are connected in a mutually beneficial relationship.

An interesting observation from our studies is that both *in situ* replication and *in situ* packaging must be perfectly coordinated to allow phages to engage in LT. This was best illustrated with P22 tsc_2*29*, where high levels of *in situ* replication were observed, but not high frequencies of LT, since most of the DNA packaging machinery was probably titrated away by the high levels of episomally replicating viral DNA. Likewise, our results also highlight the fine regulation that occurs between *in situ* packaging and late excision, which balances optimal phage reproduction with LT.

In summary, the results presented here re-write important concepts of phage biology, including the series of events that occur after lysogenic induction. Moreover, these results also have potential to fundamentally re-structure our understanding of the roles phages play in bacterial evolution, including the development of antimicrobial resistance and virulence in clinical strains.

Materials and Methods

Bacterial strains and growth conditions

Bacterial strains used in this study are listed on Table S2. *Salmonella enterica* strains were grown at 30°C, 37ºC or 42°C on Luria-Bertani (LB) agar or in LB broth with shaking (120 rpm). *Enterococcus faecalis* strains were grown at 37ºC on Brain Heart Infusion (BHI) agar or in BHI broth with shaking (120 rpm). For antibiotic selection, ampicillin (100 µg ml^{-1}), kanamycin (30 µg ml^{-1}), chloramphenicol (10 or 20 µg ml^{-1}) or tetracycline (3 or 20 µg ml^{-1}), from Sigma, was added when appropriate.

DNA methods

Gene insertions or deletions in *Salmonella* were performed as described (*31*). Briefly, the chloramphenicol (*cat*), kanamycin (*km*R) or tetracycline (*tet*A) resistance makers were amplified by PCR, with primers listed in Table S3. PCR products were introduced by transformation into the appropriate recipient strains harbouring plasmid pKD46, which expresses the λ Red recombinase, and the markers were inserted in the bacterial or phage genome. The different mutants obtained were verified by PCR. To eliminate the marker, plasmid FLP helper pCP20 was transformed into the strains containing the resistance marker insertions. Strains containing the plasmid pCP20 were grown overnight at 30°C and a 1:50 dilution (with fresh LB) was prepared and grown for 4 h at 42°C to encourage plasmid loss and produce FLP recombination. Strains were plated out on LB plates and incubated for 24 h at 37°C. Individual colonies were streaked out and PCR was performed to corroborate that the chromosomal marker had been removed and were sequenced by Sanger sequencing (Eurofins Genomics).

Insertion of a *tet*M cassette into the *E. faecalis* chromosome was performed by double recombination using allelic exchange plasmid pBT2bgal. Briefly, plasmids pJP2563, pJP2564, pJP2565, pJP2566, pJP2567 and pJP2568 were introduced into *E. faecalis* V583-derivative strains VE18990 (pp-) and VE18562 (fp1) by transformation, with selection at 32ºC on BHI

agar supplemented with 10 µg ml^{-1} chloramphenicol. Following two rounds of sequential incubation at 32°C and 42°C, as previously described (*32*), individual tetracycline-resistant, chloramphenicol-sensitive colonies were selected, and PCR was performed to confirm the correct placement of the tetracycline marker in the bacterial chromosome. Sanger sequencing (Eurofins Genomics) of PCR products corroborated marker placement.

Plasmid construction

Plasmid pJP2534 (Table S4) was generated by cloning the PCR product containing the P22 *int-xis* region, amplified with the oligonucleotides listed in Table S3 (Sigma), into the pBAD18 vector. The cloned plasmid was verified by Sanger sequencing (Eurofins Genomics).

For insertion of *tetM* into the *E. faecalis* chromosome, we made use of the thermosensitive allelic exchange plasmid pBT2bgal. Briefly, the *E. faecalis* chromosomal regions flanking the proposed *tetM* insertion site were amplified by PCR using the oligonucleotides listed in Table S3. The *tetM* cassette was amplified from plasmid pRN6680 (*33*) using the oligonucleotides indicated. Overlap extension PCR was used to produce chromosomal left flank-*tetM* fusion products, which were cloned into pBT2bgal alongside the right-flank PCR product, generating plasmids pJP2563, pJP2564, pJP2565, pJP2566, pJP2567 and pJP2568 (Table S4). All plasmid sequences were verified by Sanger sequencing (Eurofins Genomics).

Induction experiments

For *Salmonella* phage induction, overnight cultures of lysogenic donor strains were diluted 1:50 in fresh LB broth, then grown at 32°C and 120 rpm until an OD_{600} of 0.2 was reached. Prophages were induced by either addition of mitomycin C (MC) (2 µg ml^{-1}) or by shifting the temperature to 42°C (30 minutes) for thermal induction. Following induction, cultures were incubated at 32°C with slow shaking (80 rpm). Cell lysis occurred 3-4 h post-induction.

For *E. faecalis* phage induction, overnight cultures of lysogenic donor strains were diluted 1:25 into fresh BHI broth, then grown at 37°C, 120 rpm until an OD_{540} of 0.10 was reached.

Prophages were induced by addition of MC (2 µg ml^{-1}). Following induction, cultures were incubated at 32°C, 80 rpm for 5.5 h to permit cell lysis. Cell lysis occurred 4-5 h post-induction.

Infection experiments

For *Salmonella* phage infection, recipient strains were diluted 1:50 in fresh LB broth and incubated at 32°C and 120 rpm until an OD_{650} of 0.15 was reached. The culture was then centrifuged for 5 min at 4 °C/4000 rpm. The supernatant was discarded, and the pellet re-suspended at a ratio 1:1 of LB-phage buffer (phage buffer [PHB]: 1 mM NaCl, 0.05M Tris pH 7.8, 1 mM $MgSO_4$, 4 mM $CaCl_2$). The culture was then infected with a phage lysate at a ratio of 1:1 and incubated at 32°C with slow shaking (80 rpm). Generally, cell lysis occurred 4-5 h post-infection.

For *E. faecalis* phage infection, recipient strains were diluted 1:25 into fresh BHI broth, then grown at 37°C, 120 rpm until an OD_{540} of 0.34 was reached. 55 µl of recipient cells were mixed with 100 µl phage lysate diluted in PHB (2.0 x10^7 Φp1 PFU, yielding an infection ratio of 1:1), and incubated at room temperature for 10 mins before addition of 3 ml phage top agar (PTA: 20 g Nutrient broth no. 2, 3.5 g agar, 10 mM $MgCl_2$). The entire volume was poured onto phage base agar (PBA: 25 g of Nutrient Broth No. 2, Oxoid; 7g agar, Formedium) supplemented with 10mM $MgCl_2$, then incubated at 37°C for 16-18 h. Phage plaques were harvested by collecting and resuspending the PTA layer in 3 ml PHB. Samples were vortexed for 20s, then centrifuged for 10 minutes at 4000 x *g*, and the resulting supernatants were filter sterilized.

Phage lysates obtained either by infection or induction were filtered using sterile 0.2 µm filters (Minisart® single use syringe filter unit, hydrophilic and non-pryogenic, Sartonium Stedim Biotech) and the number of phage or transducing particles quantified.

Phage titration and transduction

For *Salmonella* phage titres, serial dilutions of phage lysates were prepared in PHB, and 100 µl of diluted lysate was used to infect 50 µL of cells at OD_{600} 0.34 for 10 min at room

temperature. For *E. faecalis* phage titres, serial dilutions of phage lysates were prepared in PHB, and 100 µl of diluted lysate was used to infect 55 µL of VE18590 (pp-) recipient cells at OD_{540} 0.34 for 10 min at room temperature. Following incubation, 3 ml PTA (supplemented to a final concentration of 10 mM with $CaCl_2$, for *Salmonella* phages, or $MgCl_2$, for *E. faecalis* phages) was added to stop the infection process, and the different combinations of culture:phage dilutions were plated out on PBA supplemented to a final concentration of 10 mM with either $CaCl_2$ or $MgCl_2$ as appropriate. PBA plates were incubated at 37°C for 24h and the number of plaques quantified as plaque forming units (PFU)/ml.

For transductions, a total of 1ml of *Salmonella* recipient cells at OD_{600} of 1.4 supplemented with 4.4mM of $CaCl_2$ or 1ml of *E. faecalis* recipient cells at OD_{540} of 1.4 supplemented with 4.4mM of $MgCl_2$, were infected for 30 mins at 37°C with the addition of 100 µL of phage lysate diluted in PHB. Following incubation, 3 ml LB top-agar (LTA: 20g LB, Sigma; 7.5 g agar, Formedium) or BHI top-agar (BTA: 37g BHI, Oxoid; 7.5g agar, Formedium) was added to stop the transduction process, and the entire contents were poured onto LBA (*Salmonella*) or BHI (*E. faecalis*) agar plates containing the appropriate antibiotic. Plates were incubated at 37°C for 24h (*Salmonella*) or 36h (*E. faecalis*) and the number of colonies formed (transduction particles present in the lysate) were counted and represented as the transduction forming units (TFU)/ml. Results were generally reported as the transduction units (TrU/10^9 PFU), which represents the number of transducing particles per 1E+9 of PFU.

Co-transduction analyses

The frequency of marker co-transduction was determined using lysates generated either by phage induction or by phage infection of the strains containing both resistance markers (*cat* and *tet*A), at varying distances apart. 100 *tet*A-resistant transductants were tested for *cat* resistance and the results were represented as the frequency of (*cat*/*tet*A) x 100%.

Inducible complementation of the P22 Δ*int-xis* mutant

The P22 Δ*int-xis* lysogens complemented in trans with the pBAD18 derivative plasmid expressing the *int-xis* genes were diluted 1:50 (in fresh LB broth supplemented with ampicillin at 100 μg ml^{-1}) and were grown at 32°C, 120 rpm until an OD_{600} of 0.2 was reached. Cultures were induced with MC (t=0) and incubated at 32°C with slow shaking (80 rpm). Arabinose (0.02%) was added at 0, 30, 60, 90, 120, 150, 180 and 240 min post-induction for complementation of *int-xis* functions. Cultures were filtered using sterile 0.2 μm filters and the number of phage and transducing particles in the resultant lysate were quantified.

Whole genome sequencing (*in situ* replication)

Samples were induced as described in previous sections. At the indicated time points after MC-induction, 12 ml of sample was collected and DNA extraction was performed using the 'ChargeSwitch® gDNA Mini Bacteria Kit' from Thermo Fisher Scientific, following the manufacturer's instructions. The DNA was precipitated by 0.3M NaOAc and 2.25 volume of 100% ethanol, then pelleted at 12,000 x g for 30 min at 4ºC and washed once with 1 ml of 70% ethanol. After centrifugation, the DNA pellets were air dried for 30 min and resuspended in 50 μl nuclease free water. Quality control of DNA samples was tested using Agilent Bioanalyzer 2100 and whole genome sequencing (WGS) was performed at the University of Glasgow Polyomics Facility using Illumina TruSeq DNA Nano library prep, obtaining 2x75 bp pair end reads with DNA PCR free libraries. A total of 2.2M reads were generated and trimmed reads were mapped to the appropriate genome: P22 (NC_002371.2), ES18 (NC_006949) and LT2 (NC_003197).

Whole genome sequencing (phage DNA from capsid extraction)

A total of 100 ml P22 phage lysate was produced by MC induction. Phage lysates were treated with RNase (1 µg ml^{-1}) and DNase (10 µg ml^{-1}) for 30 min at room temperature. Followed by addition of 1 M of NaCl to the lysate for 1 h on ice. After incubation, the mix was centrifuged at 11,000 x *g* for 10 min at 4°C, and phages were resuspended with 10% wt/vol polyethylene glycol (PEG) 8000 and kept overnight at 4ºC. Phages were precipitated at 11,000 x *g* for 10 min at 4°C and resuspended in 1 ml of phage buffer. The precipitated phages were loaded on the CsCl step gradients (1.35, 1.5 and 1.7 g ml^{-1} fractions) and centrifuged at 80,000 x *g* for 2h at 4°C. The phage band was extracted from the CsCl gradients using a 23-gauge needle and syringe. Phages were dialyzed overnight to remove CsCl excess using SnakeSkin™ Dialysis Tubing (3.5K MWCO, 16mm dry) into 50mM of Tris pH 8 and 150mM NaCl buffer.

Following CsCl purification, phage lysates were treated with DNase (10 µg ml^{-1}) for 30 min at room temperature and DNase was inactivated with 5mM EDTA for 10 min at 70°C. Phage lysate was combined with an equal volume of lysis mix (2% SDS and 90 µg ml^{-1} proteinaseK) and incubated at 55ºC for 1 h. DNA was extracted with an equal volume of phenol:chloroform:isoamyl alcohol 25:24:1 and samples were centrifuged at 12,000 x *g* for 5 min, and the aqueous phase containing the DNA was obtained. DNA was ethanol precipitated as already described, and the resulting DNA was resuspended in 100 µl nuclease free water.

Quality control of DNA samples was tested using Agilent Bioanalyzer 2100 and WGS was performed at the University of Glasgow Polyomics Facility using Illumina TruSeq DNA Nano library prep, obtaining 2x75 bp pair end reads with DNA PCR free libraries. A total of 3000X bacterial genome coverage, 104M reads, were generated and trimmed reads were mapped to the appropriate genome: P22 (NC_002371.2) and LT2 (NC_003197).

WGS analysis

We first used FastQC (http://www.bioinformatics.babraham.ac.uk/projects/fastqc/) to assess the quality of the sequencing reads and Trimmomatic v0.3 to remove adapters and low-quality

reads. Sequencing reads from each experiment were mapped to their respective reference genomes using the Burrows-Wheeler Alignment Tool (http://www.bioinformatics.babraham.ac.uk/projects/fastqc/). Picard-tools v2.1.1 (http://broadinstitute.github.io/picard/; Broad Institute) was next used to obtain the bam files, which were merged with SAMtools (*34*), sorted and indexed; and Bedtools *bamtobed* (*35*) was used to produce the bed files. We computed the relative coverage over 100 sliding windows along the entire chromosome for each of the experiments. For this, we computed the average coverages across the full genome without phages, which were removed using bedtools subcommand *subtract*. Subsequently, the coverages across the sliding windows were divided by the chromosomal averages. In order to estimate the percentage of integration, we calculated the number of reads that spanned the bacterial chromosome and phages on the two ends of the P22 and ES18 phages. In addition, we counted the reads that spanned chromosome-to-chromosome and reads that presented their starting and ending points on the two sides of the phage, which only correspond with circularized phages. These analyses were performed using the *view* subcommand of samtools and filtering by the coordinates of the mapping reads and their respective lengths. The integration percentages were obtained by dividing the reads chr:pha reads by the total reads (chr:pha + chr:chr).

Finally, the sequencing reads of the capsids were rarefied by subsampling 100 million reads from each of the paired, filtered reads using seqtk v1.3 *sample* command (Toolkit for processing sequences in FASTA/Q formats. Available from: https://github.com/lh3/seqtk.). Reads were mapped to the NC_003197 reference genomes and processed as above. The absolute coverage was calculated using bedtools by 100 bp windows across the entire genome. Assemblies of the content of the capsids were obtained using SPAdes v3.12 (*36*).

Total RNA extraction and mRNA enrichment

Following induction of lysogenic strains, 30 ml samples were collected at the indicated time points post-MC addition, and cell pellets were harvested by centrifugation at 5,000 x *g* for 5 min. The bacterial pellet was resuspended in TE buffer (10 mM Tris-Cl, 1 mM EDTA, pH 8.0)

containing lysozyme (50 mg ml^{-1}) and was lysed in a FastPrep-24 homogenizer (MP Biomedicals) using two cycles of 60 s at 6.5 m s-2 interrupted by a 5 minutes incubation on ice. Total RNA was extracted using a RNeasy kit (Qiagen) according to the manufacturer's instructions and genomic DNA was removed using TURBO DNase (Ambion, Carlsbad, CA, USA). RNA samples were enriched for mRNA using MICROBexpress mRNA enrichment kit (Ambion). Quality control of RNA-seq samples for mRNA enrichment was tested using Agilent Bioanalyzer 2100 at the University of Glasgow Polyomics Facility. Experiments were performed in triplicate.

RNA-seq transcriptome analysis

cDNA synthesis and sequencing, 75 bp single end reads, was performed at the University of Glasgow Polyomics Facility using Illumina NextSeq 500. The sequencing reads were processed using Trimmomatic v0.3 (*37*) for removal of adapters and low quality reads. Transcriptomic analyses were performed using the pipeline READemption v0.4.3 (*38*). First, we created individual projects for each experiment using the create subcommand and the fasta and annotation files of the reference genome (P22: NC_002371) were transferred to the corresponding locations. Next, we performed the alignment step using default parameters, and the coverage was computed using only the uniquely aligned reads, normalizing by these reads. The strand specific coverage counts normalized by 100,000 division were used for the final analyses. Strands coverage values of the phage spanning regions for different replicates were plotted with values >1 log10 corrected.

Statistical analyses

All statistical analyses were performed as indicated in the figure legends using GraphPad Prism 6.01 software. Statistical value for each experiment is listed in Table S1.

References and Notes

1. D. L. Court, A. B. Oppenheim, S. L. Adhya, A new look at bacteriophage lambda genetic networks. *J. Bacteriol.* **189**, 298–304 (2007).

2. M. M. Susskind, D. Botstein, Molecular genetics of bacteriophage P22. *Microbiol. Rev.* **42**, 385–413 (1978).

3. S. R. Casjens, The DNA-packaging nanomotor of tailed bacteriophages. *Nat. Rev. Microbiol.* **9**, 647–657 (2011).

4. V. B. Rao, M. Feiss, The bacteriophage DNA packaging motor. *Annu. Rev. Genet.* **42**, 647–681 (2008).

5. G. Streisinger, R. S. EDGAR, G. H. DENHARDT, Chromosome strcuture in phage T4. I. Circularity of the linkage map. *Proc. Natl. Acad. Sci. U.S.A.* **51**, 775–779 (1964).

6. G. Streisinger, J. Emrich, M. M. Stahl, Chromosome structure in phage t4, iii. Terminal redundancy and length determination. *Proc. Natl. Acad. Sci. U.S.A.* **57**, 292–295 (1967).

7. M. Feiss, D. A. Siegele, Packaging of the bacteriophage lambda chromosome: dependence of cos cleavage on chromosome length. *Virology*. **92**, 190–200 (1979).

8. J. W. Little, D. W. Mount, The SOS regulatory system of *Escherichia coli*. *Cell*. **29**, 11–22 (1982).

9. J. W. Little, The SOS regulatory system: control of its state by the level of RecA protease. *J. Mol. Biol.* **167**, 791–808 (1983).

10. J. W. Little, LexA cleavage and other self-processing reactions. *J. Bacteriol.* **175**, 4943–4950 (1993).

11. R. T. Sauer, M. J. Ross, M. Ptashne, Cleavage of the lambda and P22 repressors by RecA protein. *J. Biol. Chem.* **257**, 4458–4462 (1982).

12. J. W. Little, Autodigestion of lexA and phage lambda repressors. *Proc. Natl. Acad. Sci. U.S.A.* **81**, 1375–1379 (1984).

13. E. M. Phizicky, J. W. Roberts, Kinetics of RecA protein-directed inactivation of repressors of phage lambda and phage P22. *J. Mol. Biol.* **139**, 319–328 (1980).

14. X. Liu, H. Jiang, Z. Gu, J. W. Roberts, High-resolution view of bacteriophage lambda gene expression by ribosome profiling. *Proc. Natl. Acad. Sci. U.S.A*. **110**, 11928–11933 (2013).

15. S. R. Casjens, R. W. Hendrix, Bacteriophage lambda: Early pioneer and still relevant. *Virology*. **479-480**, 310–330 (2015).

16. K. Lew, S. Casjens, Identification of early proteins coded by bacteriophage P22. *Virology*. **68**, 525–533 (1975).

17. A. R. Davidson, A common trick for transferring bacterial DNA. *Science*. **362**, 152–153 (2018).

18. J. Chen *et al.*, Genome hypermobility by lateral transduction. *Science*. **362**, 207–212 (2018).

19. J. G. Frye, S. Porwollik, F. Blackmer, P. Cheng, M. McClelland, Host gene expression changes and DNA amplification during temperate phage induction. *J. Bacteriol.* **187**, 1485–1492 (2005).

20. M. L. Morse, E. M. Lederberg, J. LEDERBERG, Transduction in *Escherichia coli* K-12. *Genetics*. **41**, 142–156 (1956).

21. N. D. ZINDER, J. LEDERBERG, Genetic exchange in Salmonella. *J. Bacteriol.* **64**, 679–699 (1952).

22. Y. N. Chiang, J. R. Penadés, J. Chen, Genetic transduction by phages and chromosomal islands: The new and noncanonical. *PLoS Pathog.* **15**, e1007878 (2019).

23. M. Levine, H. O. Smith, Sequential gene action in the establishment of lysogeny. *Science*. **146**, 1581–1582 (1964).

24. V. Israel, The production of inactive phage P22 particles following induction. *Virology*. **33**, 317–322 (1967).

25. P. Youderian, P. Sugiono, K. L. Brewer, N. P. Higgins, T. Elliott, Packaging specific segments of the *Salmonella* chromosome with locked-in Mud-P22 prophages. *Genetics*. **118**, 581–592 (1988).

26. D. Y. Kwoh, J. Kemper, Bacteriophage P22-mediated specialized transduction in Salmonella typhimurium: identification of different types of specialized transducing particles. *J. Virol.* **27**, 535–550 (1978).

27. H. Wu, L. Sampson, R. Parr, S. Casjens, The DNA site utilized by bacteriophage P22 for initiation of DNA packaging. *Mol. Microbiol.* **45**, 1631–1646 (2002).

28. S. R. Casjens *et al.*, The generalized transducing Salmonella bacteriophage ES18: complete genome sequence and DNA packaging strategy. *J. Bacteriol.* **187**, 1091–1104 (2005).

29. R. Martínez-Rubio *et al.*, Phage-inducible islands in the Gram-positive cocci. *ISME J.* **11**, 1029–1042 (2017).

30. Y.-F. Tsao *et al.*, Phage Morons Play an Important Role in *Pseudomonas aeruginosa* Phenotypes. *J. Bacteriol.* **200** (2018), doi:10.1128/JB.00189-18.

31. A. Fillol-Salom *et al.*, Bacteriophages benefit from generalized transduction. *PLoS Pathog.* **15**, e1007888 (2019).

32. K. A. Datsenko, B. L. Wanner, One-step inactivation of chromosomal genes in Escherichia coli K-12 using PCR products. *Proc. Natl. Acad. Sci. U.S.A.* **97**, 6640–6645 (2000).

33. C. Ubeda *et al.*, SaPI mutations affecting replication and transfer and enabling autonomous replication in the absence of helper phage. *Mol. Microbiol.* **67**, 493–503 (2008).

34. M. Nesin *et al.*, Cloning and nucleotide sequence of a chromosomally encoded tetracycline resistance determinant, tetA(M), from a pathogenic, methicillin-resistant strain of Staphylococcus aureus. *Antimicrob. Agents Chemother.* **34**, 2273–2276 (1990).

35. H. Li *et al.*, The Sequence Alignment/Map format and SAMtools. *Bioinformatics*. **25**, 2078–2079 (2009).

36. A. R. Quinlan, I. M. Hall, BEDTools: a flexible suite of utilities for comparing genomic features. *Bioinformatics*. **26**, 841–842 (2010).

37. A. Bankevich *et al.*, SPAdes: a new genome assembly algorithm and its applications to single-cell sequencing. *J. Comput. Biol.* **19**, 455–477 (2012).

38. A. M. Bolger, M. Lohse, B. Usadel, Trimmomatic: a flexible trimmer for Illumina sequence data. *Bioinformatics*. **30**, 2114–2120 (2014).

39. K. U. Förstner, J. Vogel, C. M. Sharma, READemption-a tool for the computational analysis of deep-sequencing-based transcriptome data. *Bioinformatics*. **30**, 3421–3423 (2014).

40. R. C. Matos *et al.*, Enterococcus faecalis prophage dynamics and contributions to pathogenic traits. *PLoS Genet.* **9**, e1003539 (2013).

41. L. M. Guzman, D. Belin, M. J. Carson, J. Beckwith, Tight regulation, modulation, and high-level expression by vectors containing the arabinose PBAD promoter. *J. Bacteriol.* **177**, 4121–4130 (1995).

42. N. Carpena, K. A. Manning, T. Dokland, A. Marina, J. R. Penadés, Convergent evolution of pathogenicity islands in helper cos phage interference. *Philos. Trans. R. Soc. Lond., B, Biol. Sci.* **371**, 20150505 (2016).

43. E. Charpentier *et al.*, Novel cassette-based shuttle vector system for gram-positive bacteria. *Appl. Environ. Microbiol.* **70**, 6076–6085 (2004).

Acknowledgements

This work was supported in part by the Singapore Ministry of Education MOE2017-T2-2-163 and MOE2019-T2-2-162 to J.C.; and by MR/M003876/1, MR/V000772/1 and MR/S00940X/1 from the Medical Research Council (UK), BB/N002873/1, BB/V002376/1 and BB/S003835/1 from the Biotechnology and Biological Sciences Research Council (BBSRC, UK), ERC-ADG-2014 Proposal n° 670932 Dut-signal (from EU), to J.R.P; and Wellcome Trust 201531/Z/16/Z to J.R.P.

Author Contributions: J.C. and J.R.P. conceived the study. A.F-S, S.H. and Y.N.C., conducted the experiments. R.B. performed the genomic and transcriptomic analyses. J.C. and J.R.P. wrote the manuscript.

Data access: All data and code to understand and assess the conclusions of this research are available in the main text, supplementary materials and via the following repository: EBI accession XXXXX.

Competing interests: Authors declare no competing interests.

List of Supplementary Materials:

Materials and Methods

Figures S1-S8

Tables S1-S4

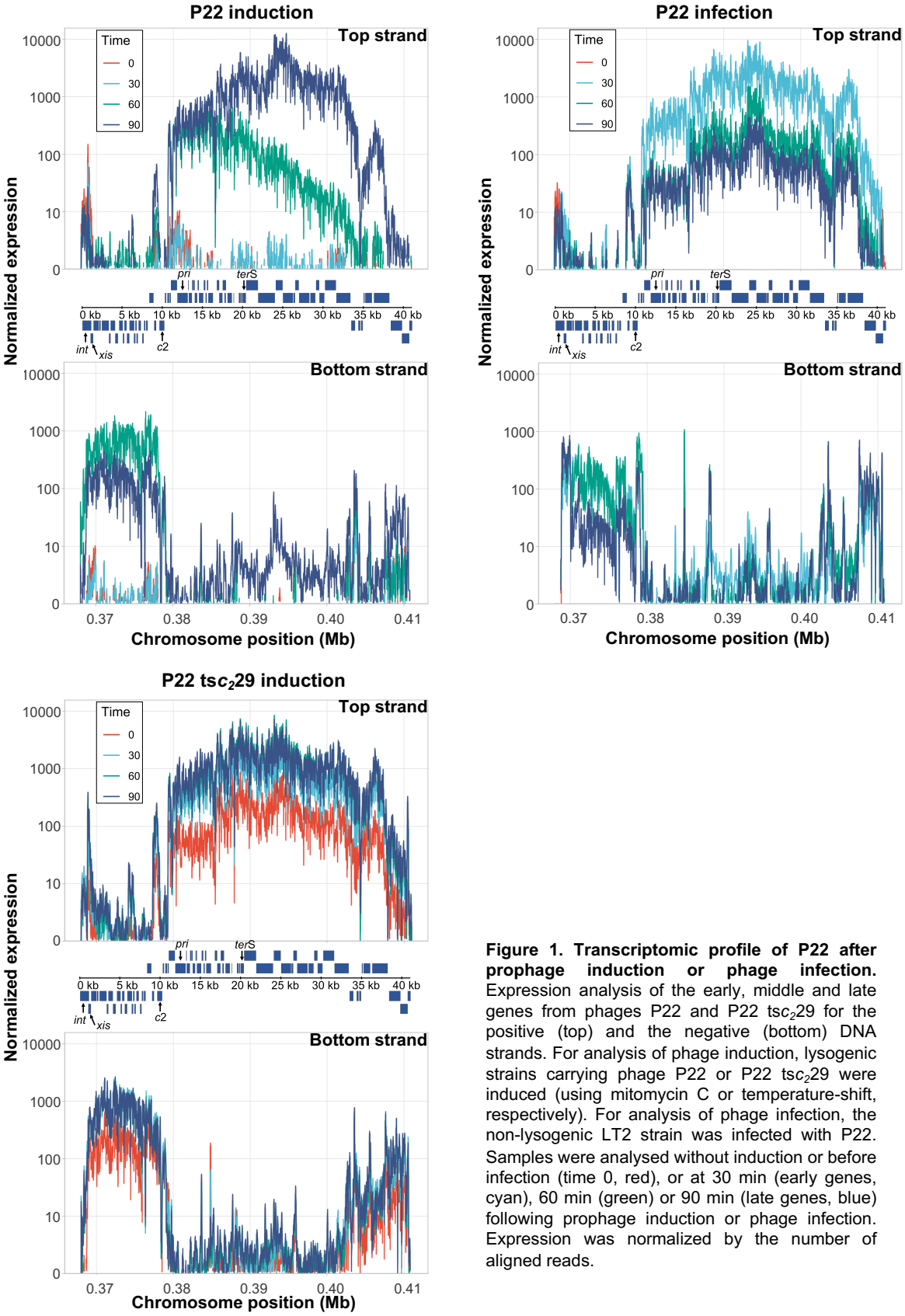

Figure 1. Transcriptomic profile of P22 after prophage induction or phage infection. Expression analysis of the early, middle and late genes from phages P22 and P22 tsc$_2$29 for the positive (top) and the negative (bottom) DNA strands. For analysis of phage induction, lysogenic strains carrying phage P22 or P22 tsc$_2$29 were induced (using mitomycin C or temperature-shift, respectively). For analysis of phage infection, the non-lysogenic LT2 strain was infected with P22. Samples were analysed without induction or before infection (time 0, red), or at 30 min (early genes, cyan), 60 min (green) or 90 min (late genes, blue) following prophage induction or phage infection. Expression was normalized by the number of aligned reads.

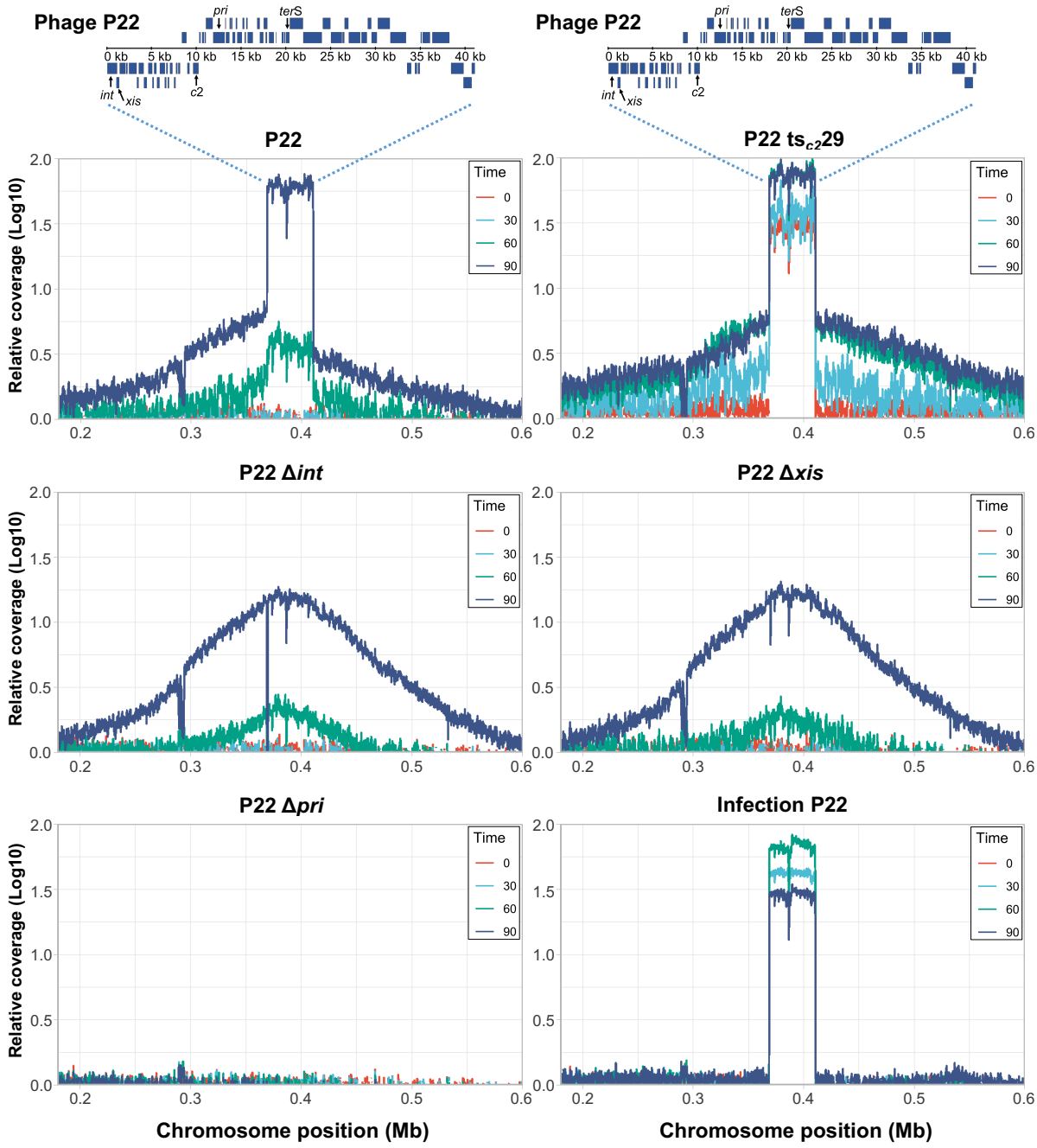

Figure 2. Phage P22 replicates *in situ* before excision. Relative abundance of phage genomic DNA and the chromosomal regions proximal to where they integrate for P22, P22 ts$c_2$29, P22 Δ*int*, P22 Δ*xis* or P22 Δ*pri* is represented. Samples were analyzed at 0 (red), 30 (cyan), 60 (green), and 90 min (blue) after induction of prophages (using mitomycin C or temperature-shift, as appropriate) or after phage infection. Relative coverage is the DNA relative to the average bacterial genomic coverage (excluding phages).

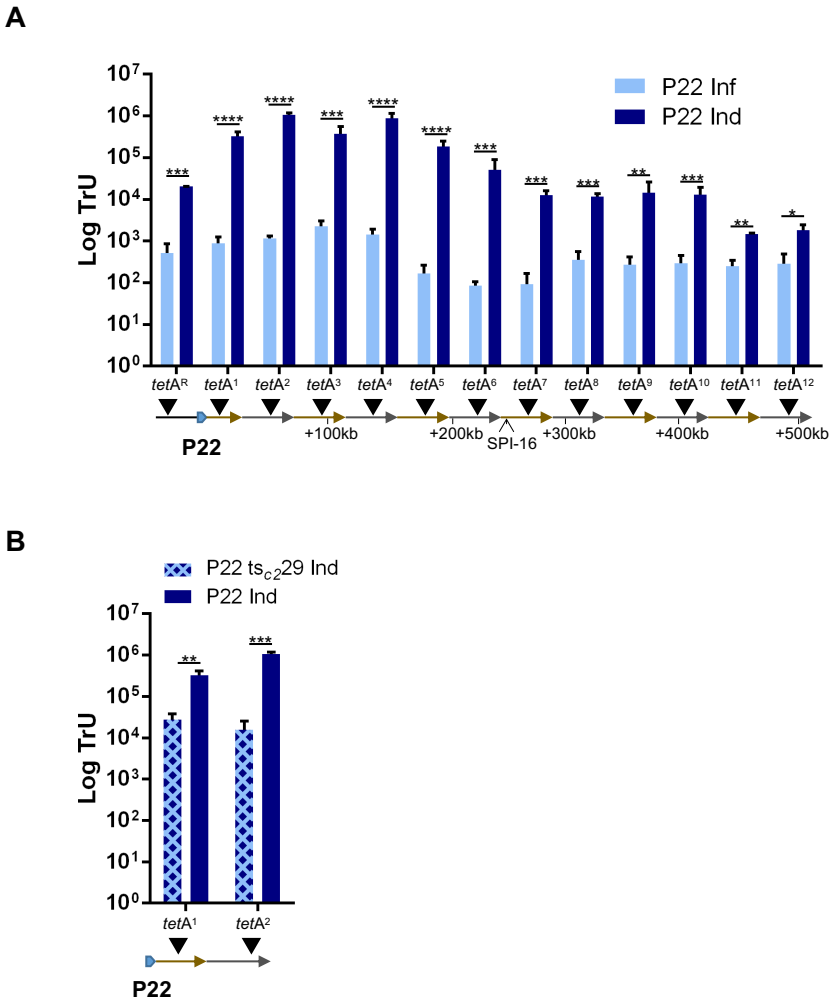

Figure 3. P22 engages in lateral transduction, transferring large metameric spans of the bacterial chromosome at high frequencies. (A) The transfer of *tet*A markers located upstream (*tet*A^{R}) or downstream of the P22 *att*B site, in twelve successive capsid headfuls (*tet*A^{n}), was tested following P22 prophage induction or P22 infection. **(B)** The transfer of the two first *tet*A markers located downstream of the P22 *att*B site was analyzed for both the P22 and the P22 ts$_{c2}$29 prophages following induction. Transduction units (TrU) per milliliter were normalized by PFU per milliliter and represented as the log TrU of an average phage titre (1 x 10^9 PFU). Error bars indicate standard deviation. For all panels, values are means (n = 3 independent samples). An unpaired t-test was performed to compare mean differences in each marker. Adjusted p-values were as follows: *ns*>0.05; *p≤0.05; **p≤0.01; ***p≤0.001; ****p≤0.0001. The exact statistical values for each of the conditions tested are listed in Table S1.

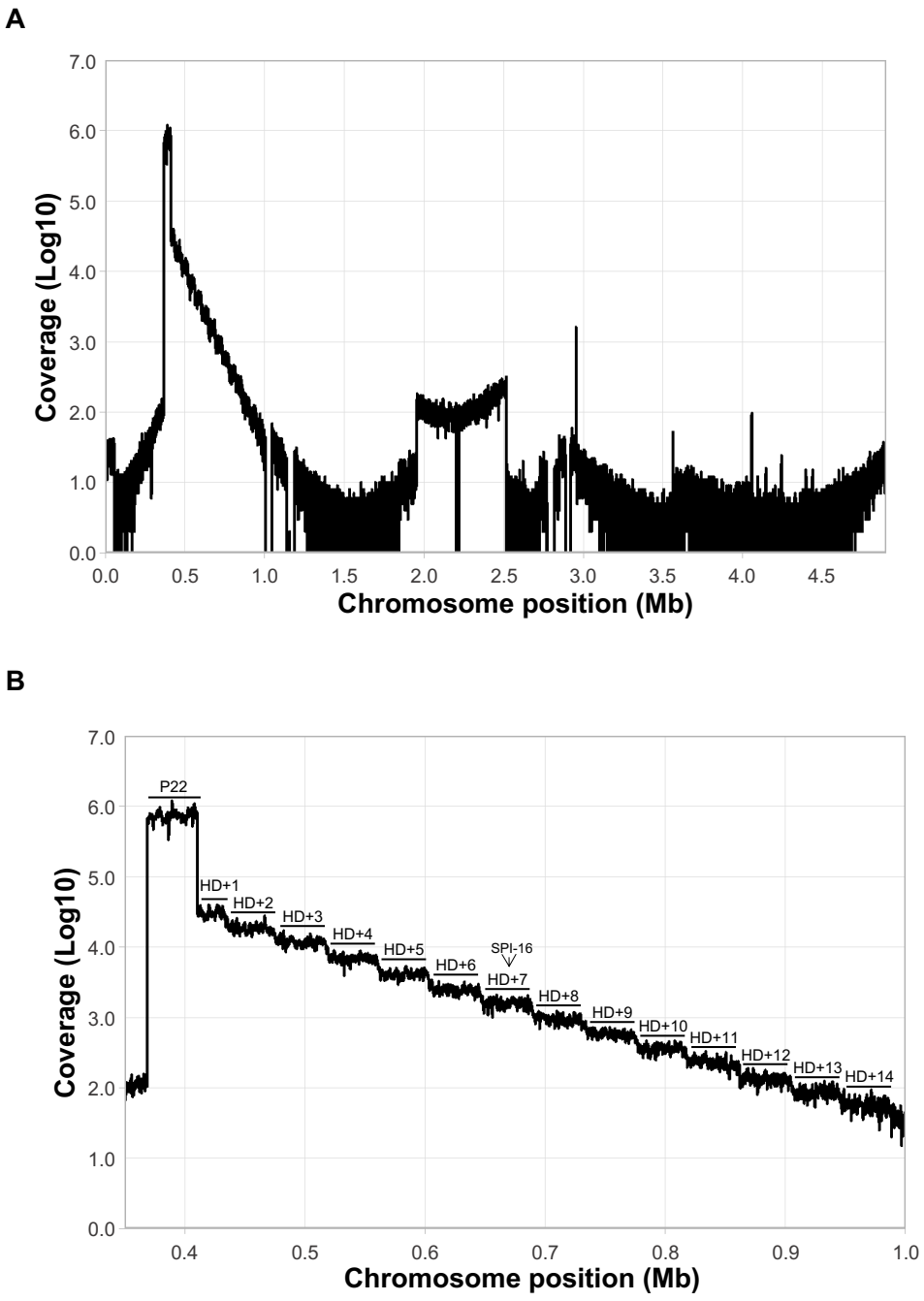

Figure 4. Capsid DNA extraction from purified P22 phage particles. (A) A P22 lysogen was mitomycin C-induced and the resulting phage particles purified. The DNA from the phage particles was extracted and sequenced. The coverage of chromosomal DNA is represented. **(B)** Zoom of the region encompassing lateral transduction is visualised, displaying a successive 'step-down' pattern in DNA packaging efficiency for each consecutive headful.

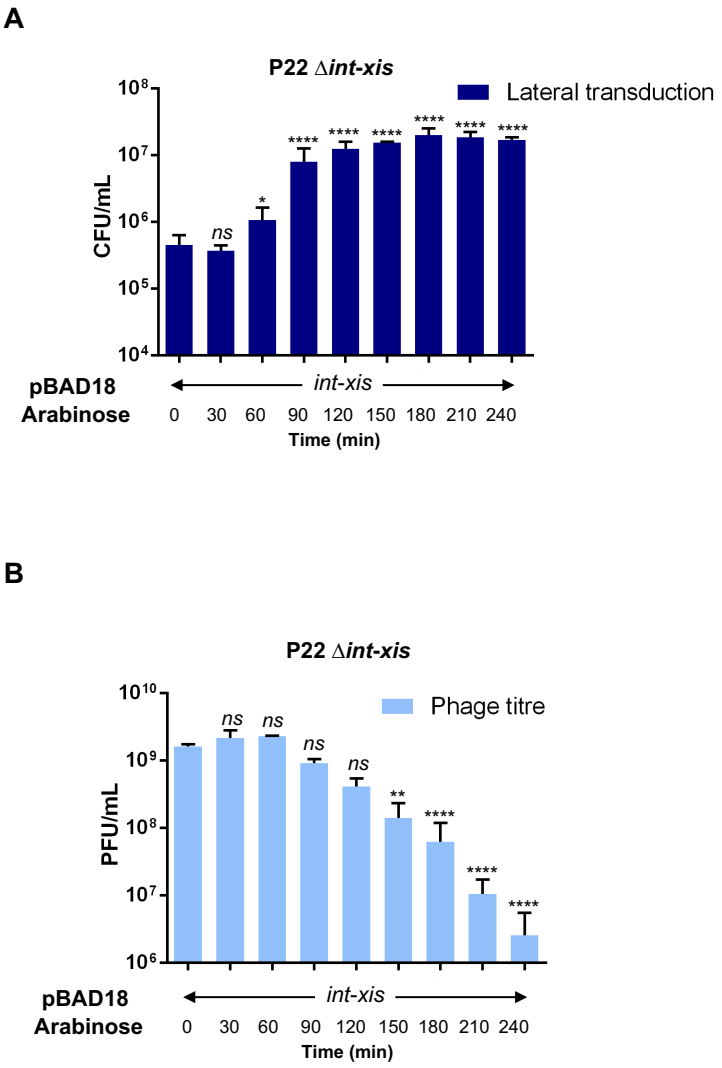

Figure 5. Effect of early or delayed excision on lateral transduction and phage formation. The lysogenic strain for phage P22 mutant Δ*int-xis,* carrying a plasmid expressing the *int* and *xis* genes, was mitomycin C-induced to activate the prophage, and arabinose (0.02%) was added at different time points to facilitate *int-xis* expression *in trans*. Lysates were tested for transduction of the *tet*A marker **(A)** and to determine the phage titre **(B)**. Error bars indicate standard deviation. For all panels, values are means (*n* = 3 independent samples). A one-way ANOVA with Dunnett's multiple comparisons test was performed to compare time 0 against the other time points. Adjusted *p*-values were as follows: *ns*>0.05; *p≤0.05; **p≤0.01; ***p≤0.001; ****p≤0.0001. The exact statistical values for each of the conditions tested are listed in Table S1.